Chapter 8

Formulation optimization and characterization of Ziprasidone nanosuspension

8.1 INTRODUCTION

The use of nanosuspensions in parenteral drug delivery is a relatively new venture. Generally, the coarse suspensions having particle size of 10μm-100μm are formulated for intramuscular and subcutaneous administration of drugs with poor aqueous solubility. Formulation of parenteral dosage forms for drugs with poor aqueous solubility has always been challenging and has been associated with many side effects (Kipp JE, 2004). Nanosuspensions have many potential advantages when used via the parenteral route. Nanosuspensions of solid drug facilitate the delivery of larger amounts of drug at lower toxicity than would otherwise be possible by micellar dispersions or solutions (Peters K et al., 2000).

Several methods have been reported for the manufacturing drug nanosuspensions such as, supercritical process (Rogers TL et al., 2001), cryogenic spraying process (Rogers TL et al., 2001), solvent evaporation (Sarkari M et al., 2002), high pressure homogenization (Keck CM and Muller RH., 2006) and wet-grinding in agitated grinding media mills (Liversidge ME et al., 2003). Wet grinding technique provides many advantages such as the avoidance of organic solvents, possibility of scale up (Keck CM and Muller RH., 2006) and reduction in the processing time. Liversidge and co workers (Liversidge ME et al., 2003; Liversidge GG et al, 1992) were able to generate drug nanosuspensions with a median diameter of less than 200nm within 1 hour. Large scale production units for pearl milling can be accomplished by circulating the suspension through the pearl mill. Surprisingly, despite of various advantages, the literature on the studies assessing the feasibility of nanosuspensions for parenteral use is limited. Herewith we describe the feasibility of this approach for the preparation of Ziprasidone (ZB) for parenteral delivery.

ZB is a chlorooxyindole class aryl heterocyclic and is normally prescribed for the treatment of schizophrenia. It is an atypical antipsychotic and atypical antipsychotics have the advantages over the traditional typical antipsychotics as they are associated with lower incidence of side effects and the absence of extra pyramidal side (EPS) effects. It has been estimated that about 30-40% of an oral dose is being converted to inactive metabolites prior to entry into the systemic circulation. After intramuscular administration, a much greater fraction of an intramuscular dose of unchanged ziprasidone enters the systemic circulation, since first-pass effect is reduced. ZB has an apparent pKa 6.5 and a very low intrinsic solubility of 0.3μg/ml.

ZB is available (its mesylate salt) in the market for parenteral administration, (Pfizer's GEODON®) which uses a concentration of 40% w/v solution of CAPTISOL® (sulfobutyl ether beta cyclodextrin) for dissolving 20 mg/ml of ziprasidone. The maximum daily parenteral dose of 40 mg of ZB results in a 588 mg exposure of CAPTISOL®. Solubility of the complex and viscosity of the resulting formulation limit the feasible concentration of cyclodextrin, and only a fixed solubility enhancement can be obtained at this high level. Normally, an excess of cyclodextrin than what is actually required as per the molar ratio is added to drive the equilibrium toward complexation (Kipp JE., 2004). This leads to higher exposure of the body to high amounts of sulfobutylether derivative of β–cyclodextrin. To avoid this, a new form of ZB with improved solubility characteristics may be required for safe intramuscular administration.

In the present chapter, the nanosuspensions of ZB were prepared and characterized. The nanosuspensions were also subjected to stability evaluation at different storage conditions. The pharmacokinetics and biodistribution studies were also performed for the nanosuspensions to assess their potential for intramuscular administration (Chapter 10).

8.2 METHODS AND METHODS

Materials

Ziprasidone base (ZB) was received as a gift sample from Cadila Healthcare, India. Poloxamer 407 was received as a free gift sample from BASF, USA. Zirconium oxide beads of diameter 0.4-.0.7 mm and 1.2-1.4mm were purchased from S.D Fine Chemicals, India. All other chemicals used in the study were of analytical grade. Water used in all the studies was distilled and filtered through 0.22 μm nylon filter before use.

Methods

Preparation and optimization of ZB Nanosuspensions

ZB nanosuspensions were prepared by pearl milling technique (Verhoff F et al., 2003). Briefly, 100 mg of poloxamer was dissolved in 10 ml of distilled water in a 20 ml glass vial. 400 mg of Zirconium oxide beads (75:25 ratio of size 0.4- 0.7mm: 1.2-1.4mm) was added (40%w/v of the batch size). 500 mg of ZB was added to the above milling chamber. Milling was initiated by magnetic stirring at 5000 rpm for 8 hours. The nanosuspension was obtained in a powder form

by either lyophilization (ZBLNS) using 1:3 (with respect to total solid content) sucrose as cryoprotectant or spray drying (ZBSNS) using 1:5 (with respect to total solid content) sucrose as cryoprotectant. Spray drying was performed at an inlet temperature of 100°C and an outlet temperature of 55°C. Spraying was performed at an inlet air pressure of 2.5 kg/cm^2 and aspiration rate of 1260CFM. The flow rate was maintained at 3 mL/min.

Assay of ZB in the ZB nanosuspensions

Both ZBLNS and ZBSNS were weighed and dissolved in Tetra hydro Furan and the solutions were analyzed using a UV – Visible spectrophotometer (Hitachi U2000, Japan) at the λ_{max} of 317 nm.

Characterization of Nanosuspensions

A. Determination of saturation solubility

The saturation solubility of ZB and both ZBLNS and ZBSNS in phosphate buffer (PB pH 7.4) was determined by adding excess material in pH 7.4 PB and mechanical shaking for 24 h to attain dissolution equilibrium. After 24 h, the dispersion was centrifuged at 15,000 rpm for 20 minutes in a cooling centrifuge (Sigma, Osterode, Germany) to sediment the undissolved drug. The absorbance of the supernatant was determined at 317nm using a UV–Visible spectrophotometer (Hitachi U2000, Japan).

B. Measurement of size and zeta potential of ZB nanosuspensions

Size and zeta potential of the nanosuspensions were measured by photon correlation spectroscopy (PCS) using Malvern Zetasizer ZS (Malvern Instruments, UK). Samples were diluted appropriately with distilled water pre-saturated with ZB (in order to avoid reduction in particle size during dilution) for the measurements.

C. Differential Scanning Calorimetry (DSC)

DSC analysis was carried out using a Differential scanning calorimeter (DSC-60, Shimadzu, Japan) at a heating rate of 10°C per minute in the range of 30°C to 250°C under inert nitrogen atmosphere at a flow rate of 80ml/min. DSC thermograms were recorded for ZB, ZBLNS and ZBSNS.

D. X- ray diffraction studies (XRD)

Powder X-ray diffraction patterns were obtained using an X-ray diffractometer (Philips PW 1710) with Cu Kα radiation generated at 30 mA and 40 kV. The source of X - ray was copper anode with a wavelength of 1.54060 Å. The XRD patterns were recorded for ZB, ZBLNS and ZBSNS.

E. Transmission Electron Microscopy (TEM) studies

TEM studies were performed in transmission electron microscope (Philips Morgagni 268). Nanoparticles were dispersed in de ionized water and one drop of the reconstituted nanoparticles was incubated on 200 – mesh carbon coated copper grid. The copper grid was fixed into sample holder and placed in vacuum chamber of the transmission electron microscope and observed under low vacuum (10^{-3} torr)

F. Determination of in vitro steric stability by electrolyte induced flocculation test

The electrolyte induced flocculation test was performed for the ziprasidone nanodispersions stabilized with 0.5% poloxamer 407. The effect of poloxamer 407 on the ability of the nanoparticle to resist electrolyte induced flocculation was investigated by this test. Sodium sulphate solutions ranging from 0 M to 1.5 M were prepared in 16.7 %w/v sucrose solution (Subramanian N et al., 2003). An appropriate volume of nanodispersion was made up to 5 ml using the sodium sulphate solutions of varying concentrations (0 M,0.3 M,0.6 M,0.9 M,1.2 M and 1.5 M) to obtain a final concentration of 1mg/ml ZB. The absorbance of the resulting dispersions was measured within 5 min at 400 nm using a UV–Visible spectrophotometer (Shimadzu, Japan) against respective blank.

G. Stability studies - Effect of Storage temperature

Short-term stability studies were conducted for the ZBLNS and ZBSNS dispersions for a period of six months. The particle size and zeta potential of the ZB nanosuspension immediately after milling was measured. Then this batch was divided into three portions and stored in transparent glass vials (USP type I) under different temperature conditions of 4°C (in a refrigerator), 30°C (ambient room temperature) and 40°C (temperature regulated oven) in a black colored box. Samples after 1, 2, 3 and 6 months were subjected to particle size and zeta potential measurements. Stability studies were conducted for the ZB nanosuspension in the

powder also. Samples after 1, 2, 3 and 6 months were subjected to particle size analysis, time for reconstitution was determined and in vitro release pattern was also determined.

H. In vitro release studies

In vitro release of ZB from the nanosuspensions (both ZBLNS and ZBSNS) was determined in pH 7.4 PB containing 2% sodium lauryl sulphate (SLS). The ZB nanosuspension was placed in a dialysis bag (cutoff molecular weight of 12000 Daltons, Himedia, India) and sealed at both ends. The dialysis bag was then dipped into the receptor compartment containing the dissolution medium. The release of ZB from ZB dispersion in PB pH 7.4 (as control) through the dialysis bag was also studied in both the media. The dissolution media was continuously stirred at 100 rpm and maintained at 37 ± 2°C. Samples were withdrawn at regular time intervals and the same volume was replaced with fresh dissolution medium. All the dissolution samples were analyzed spectrophotometrically at 317 nm against a solvent blank for drug content. All experiments were repeated thrice and the average values were taken.

8.3 RESULTS AND DISCUSSION

Influence of milling time

The initial particle size of bulk ZB was 9.73 ± 0.40μm with a broad size distribution (Figure 8.1). Pearl milling for 8 h in the presence of poloxamer resulted in smaller sized particles with mean particle diameter of 0.309 ± 0.01μm (uniformity value 0.202). Further milling beyond 8 h did not result in significant reduction in particle size (Particle size after 12 hours pearl milling 0.304 ± 0.02μm). The effect of volume of milling media, ratio of small beads to big beads and milling time on the means particle size diameter of the nanosuspension are shown in table 8.1, 8.2 and 8.3 respectively.

Erosion of the milling material and consequent contamination of the product with residues of milling media is always a considerable problem when milling techniques are used. Hence, the contamination level of milling media, zirconium in the final nanosuspension dispersion was determined by atomic absorption spectroscopy. The residual amount of zirconium in the final nanosuspension was detected to be as low as 21 ppm. The contamination levels of the milling media generally depend upon the hardness of the drug and the milling material and also the

time required for milling time which usually ranges from hours or up to several days. (Keck CM and Muller RH., 2006).

Particle size reduction is usually determined by stress intensity and the number of contact points. The stress intensity is a function of the kinetic energy of the grinding beads, and the number of contact points can be increased by utilizing smaller grinding media. However, the contamination of pharmaceutical materials by fragments of grinding media is a common problem associated with media milling technique. Various attempts have been made to keep the level of contamination at the minimum or under acceptable levels. In contrast, in some cases, the selection of grinding media was found to be not critical (Liversidge GG et al., 1992). As per the earlier report (Liversidge GG et al., 1992), zirconium oxide stabilized with magnesia, zirconium silicate, and glass grinding media provided nanosuspensions having levels of contamination which are believed to be acceptable for the preparation of pharmaceutical compositions.

Similar studies (Liversidge ME et al., 2003) using small plastic grinding media, resulted in generation of drug particle formulations having a median diameter less than 200 nm and low contamination of the formulation by the milling media (50 ppm). Further, an improved construction was suggested by Czekai and co coworkers in their US patent application to reduce this contamination by the milling media (Czekai DA and Reed RG., 2001). They claim that their improved construction is able to reduce the contaminations by mill parts (iron, molybdenum, chromium and nickel) to less than 10 ppm and by grinding media (plastic) to less than 1000 ppm. This method has been described as NanoCrystal® technology and has already found industrial application for the drugs Rapamune® by Wyeth and Emend® by Merck (Coppola D., 2003).

The nanosuspensions were found to be unstable in the dispersion state, and hence their recovery in the powder form is essential to improve the stability. The nanosuspension dispersion was recovered in the powder form either by lyophilization or spray drying. Lyophilization was carried out using 1:3 (with respect to total solid content) sucrose as cryoprotectant. Nanosuspensions lyophilized with lesser quantities of sucrose resulted in particle size growth. Sucrose was added to the nanosuspension dispersion to obtain the drug

dispersed in an inert material. Simultaneously, the sucrose also aids in the dispersitivity of the nanoparticles in the reconstitution medium. Lyophilization was widely primarily used for this purpose and was also reported to improve the stability in case of clofazimine nanosuspension for intravenous use (Peters K et al., 2000). In the present study, we used the spray drying technique and proved to be very convenient method to transfer the drug nanosuspension dispersion into dry powder form. Spray drying was done by adding 1:5 (with respect to total solid content) sucrose as cryoprotectant. Nanosuspensions spray dried with less than the above mentioned sucrose ratio lead to powders which were hygroscopic in nature. Spray drying technique can be favored lyophilization because it is cost-effective, especially beneficial for large-scale purposes and widely acceptable.

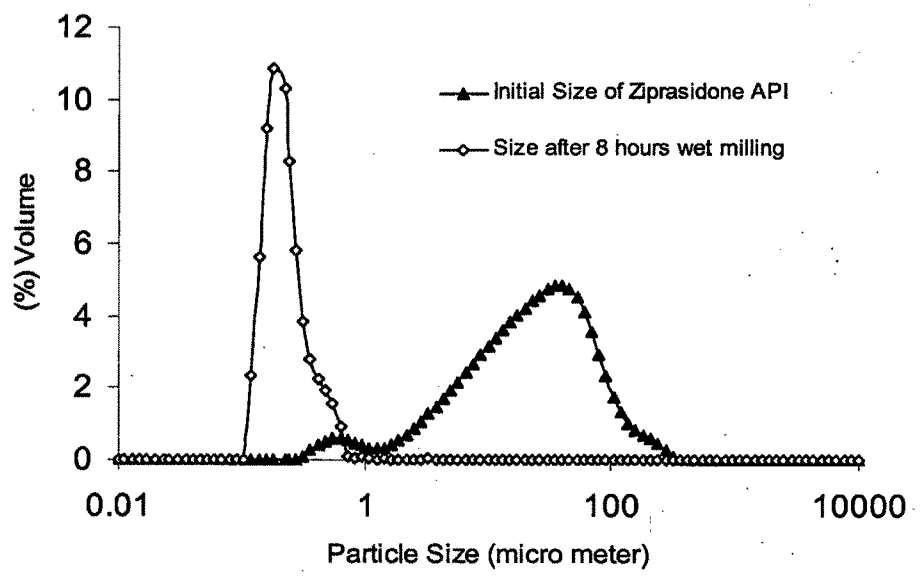

FIGURE 8.1: Particle size distribution of Ziprasidone before and after media milling.

Volume of beads (%w/v)	Mean Particle Size diameter ± S.D (nm)	Uniformity value
25	470 ± 5.87	0.520
30	411 ± 3.85	0.438
35	337 ± 5.02	0.287
40	309 ± 4.28	0.202
45	306 ± 5.68	0.185
50	305 ± 4.04	0.227

TABLE 8.1: Effect of volume of beads on the particle size of ziprasidone nanosuspension (milling time: 8 hours; using 0.4-0.7mm zirconium beads)

Ratio of beads (0.4mm–0.7mm:1.2mm–1.4mm)	Mean Particle Size diameter ± S.D (nm)	Uniformity value
0 : 100	503 ± 4.63	0.412
25 : 75	428 ± 3.37	0.338
50 : 50	440 ± 2.88	0.334
75 : 25	309 ± 4.28	0.202
100 : 0	425 ± 3.06	0.353

TABLE 8.2: Effect of ratio of beads on the particle size of ziprasidone nanosuspension (milling time: 8 hours; Volume of beads maintained at 40%w/v)

Milling Time (hours)	Mean Particle Size Diameter ± S.D (nm)	Uniformity value
Initial	9730 ± 206.33	1.610
0.5	6452 ± 87.08	1.451
1	2098 ± 52.42	1.032
2	1085 ± 29.67	0.776
4	570 ± 11.63	0.442
8	309 ± 4.28	0.202
12	304 ± 2.88	0.224

TABLE 8.3: Effect of milling time on the particle size of ziprasidone nanosuspension (Volume of beads – 40%w/v; using 75:25 ratio of 0.4mm–0.7mm: 1.2mm–1.4mm zirconium beads)

Differential Scanning Calorimetry

The crystalline structure of the nanosuspensions can be assessed by differential scanning calorimetry (DSC). This is especially important when a drug exists in different polymorphic forms. The DSC curves for the bulk ZB, ZBLNS and ZBSNS are shown in figure 8.2a, 8.2b and 8.2c.

The DSC curve of ZB base (Figure 8.2a) showed a melting endotherm of the drug at 226.64°C. This peak was found absent in the thermograms of ZBLNS and ZBSNS (Figure 8.2b and 8.2c). A melting endotherm was observed at 206.87°C for ZBLNS and 209.52°C for ZBSNS. Further this melting endotherm was not observed as a distinct, sharp transition. This indicates the presence of ZB in an amorphous state. This may be attributed to increased lattice defects in the drug crystal, which in turn reflects reduced degree of crystallinity as a result of pearl milling. Formation of another polymorphic form is also possible as Otsuka and co workers during ball milling observed polymorphic transformations of chloramphenicol palmitate (Otsuka M and Kaneniwa N., 1986). The DSC results are represented in table 8.4.

Crytallinity index was determined by the enthalpy of the bulk drug as 100% (Saupe A et al., 2005). The crytallinity index was found to be 63.44% and 37.81% for ZBLNS and ZBSNS respectively. The low crystallinity index observed with ZBSNS indicates the advantage associated with spray drying.

The long milling operation times may also sometimes induce the formation of amorphous domains in crystalline starting material which is not desired. Hydration of these regions may lead to instability, either during subsequent processing or upon storage of the final product. This effect was observed in the jet milling of albuterol sulfate (Ward GH and Schultz RK., 1995). Crystalline to amorphous transitions have also been observed in the ball milling of some organic compounds (Willart JF et al., 2001; Font J et al., 1997). Such transitions like conversion of crystalline domains to amorphous domains and polymorphic transformations not only can alter physical characteristics of a drug, but also its in vivo performance as well. Chloramphenicol palmitate undergoes polymorphic transformation from its desired metastable form (Form B) to Form A by temperature or by seeding (Byrn SR et al., 1999). Ball milling has also been found to induce this polymorphic conversion (Otsuka M and Kaneniwa N., 1986).

Generally for a given compound, the polymorph with the closest packing (and greater density) will have a higher heat of fusion (and melting point), and lower solubility. Kitaigorodkii proposed that increased packing density lowers solid enthalpy (Kitaigorodkii, 1961). Wallach's rule, later confirmed by Brock and co workers, says that racemic solids are generally denser than the individual enantiomeric crystals are therefore considered to be more stable (Brock CP et al., 1991). However, exceptions also exist due to the presence of other factors such as hydrogen bonding and lattice symmetry (Byrn SR et al., 1999).

DSC Parameters	Bulk Ziprasidone	Ziprasidone Nanosuspension	
		ZBLNS	ZBSNS
Enthalpy	120.92 J/g	76.72	45.73
Onset	224.28°C	205.12	208.60°C
Peak	226.64°C	206.87	209.52°C
Crytallinity Index	100.00%	63.44%	37.81%

TABLE 8.4: Differential scanning calorimetry data of Bulk Ziprasidone and both lyophilized and spray dried nanosuspension.

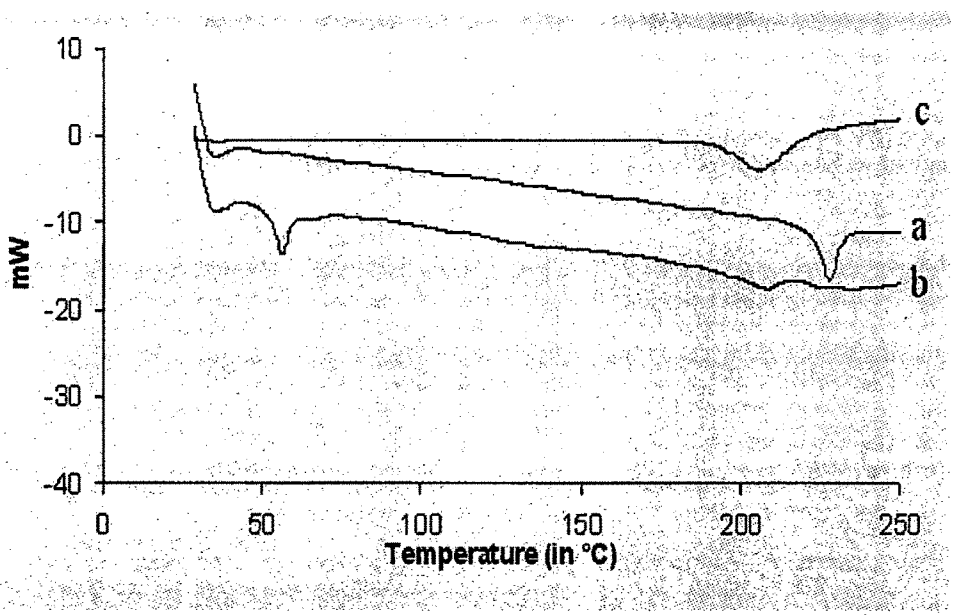

FIGURE 8.2: Differential Scanning Calorimetry thermograms of Ziprasidone (a) and Ziprasidone spray dried nanosuspension (b) and Ziprasidone lyophilized nanosuspension (c)

Powder X- ray diffraction studies (PXRD)

Crystal diffraction software tools are widely used to simulate PXRD patterns as reference standards for individual crystal forms (such as polymorph, solvates, and salts). The small differences between observed and simulated PXRD patterns, such as the appearance of new peak(s), additional shoulders, shifts in the peak position, or abnormal intensity distribution, can indicate the presence of different forms (e.g. polymorphs, solvates). The XRD diffraction patterns for the bulk ZB, ZBLNS and ZBSNS are depicted in figure 8.3a, 8.3b and 8.3c. Comparison of the XRD patterns was done by considering the relative intensities of the diffracted peaks and inters planar spacing d. The relative intensity is defined by the ratio of the peak intensity of a particular diffraction angle to the intensity of the standard peak. The diffraction peak with the strongest maxima is usually considered as the standard peak. The XRD pattern of ZB base showed a total of 48 peaks while the XRD patterns of ZBLNS and ZBSNS showed a total of 33 and 32 peaks respectively. The standard peak in ZB was found at a diffraction angle (°2θ) of 24.855 with a d value of 3.5794 Å. In the XRD pattern of ZBLNS, the standard peak was found at a diffraction angle of 20.030 with a d value of 4.4294 Å and in ZBSNS, the standard peak was found at a diffraction angle of 19.940 with a d value of 4.4492 Å. These values indicate the possible change in crystal form of ZB in both ZBLNS and ZBSNS. The crystallinity index of ziprasidone after conversion into nanosuspension was calculated by considering the intensity of the principle peak obtained with bulk ziprasidone as 100%.

Formulation	Peak intensity at angle 20.030 °2θ [counts]	Crystallinity index (%)
Bulk Ziprasidone	1149	100.00
ZBLNS	404	35.16
ZBSNS	488	42.47

TABLE 8.5: X - ray diffraction data of bulk ziprasidone and both ziprasidone nanosuspensions

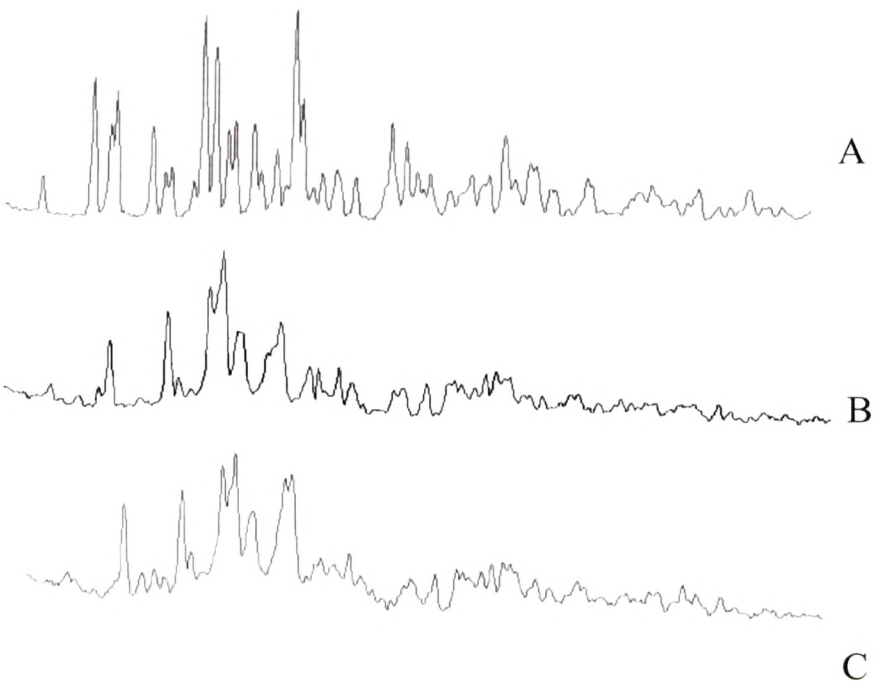

FIGURE 8.3: X – ray diffraction pattern of Ziprasidone (A) Ziprasidone lyophilized nanosuspension (B) and Ziprasidone spray dried nanosuspension (C)

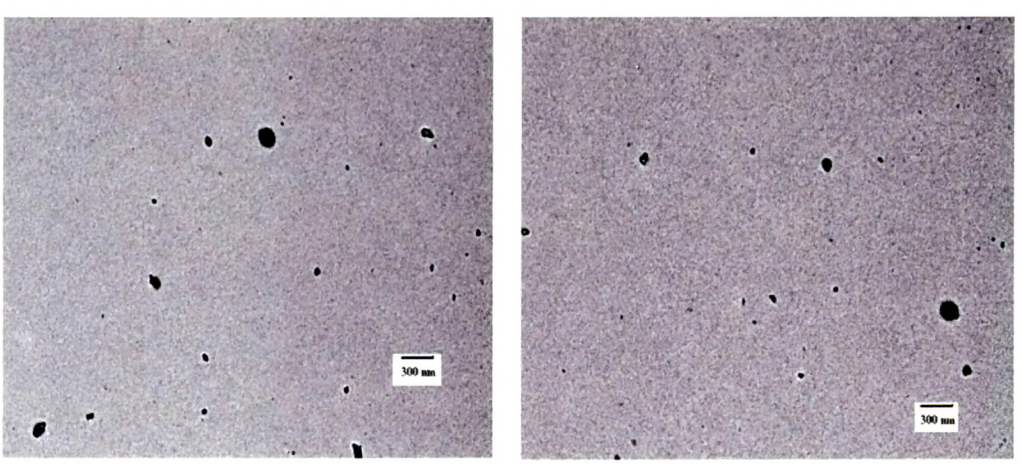

A **B**

FIGURE 8.4: Transmission electron micrograph of ZBLNS (A) and ZBSNS (B)

Determination of in vitro steric stability by electrolyte flocculation test

The effect of poloxamer 407 on the ability of the nanoparticles to oppose electrolyte induced flocculation was investigated by this test. Coating the particulate systems with hydrophilic surfactants provide steric stability by rendering a hydrophilic surface, which in turn reduces the binding of serum opsonins and also cells of the reticuloendothelial system (Huang SK et al., 1993). Addition of electrolyte compresses the electrical double layer around the particle. This results in flocculation of the particles with a corresponding increase in optical turbidity of the particle dispersion which can be measured by the absorbance of the dispersion at 400nm. The scattering of the sample increased by the inverse 4^{th} power of the wavelength of the incident light, and hence authors used a lower wavelength (400nm) was used for the measurements (Subramanian N et al., 2003).

In the present investigation, the nanoparticle formulations stabilized with 0.5%w/v poloxamer 407 showed a gradual increase in the flocculation as the concentration of electrolyte (sodium sulphate) was increased. The nanodispersions showed signs of flocculation when the concentration of sodium sulphate was increased above 0.3M. Beyond this concentration, a sharp increase in the flocculation was observed. The results are given in figure no 8.5.

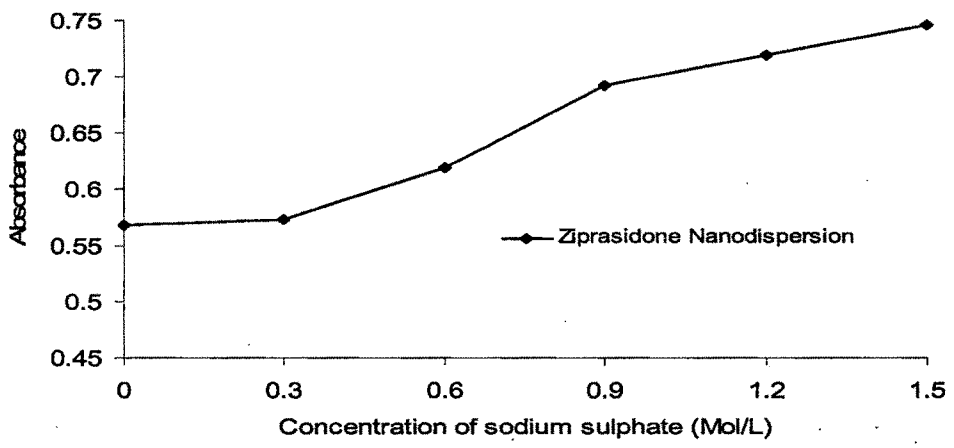

FIGURE 8.5: Steric stabilization effect of the ziprasidone nanosuspension. The nanoparticles were stabilized by 0.5% w/v of Poloxamer 407.

Saturation Solubility

The saturation solubility of bulk ZB in pH 7.4 PB was 0.26 ± 0.02μg/ml. The solubility of ZB increased considerably upon formulating as nanosuspension. The saturation solubility of ZBLNS and ZBSNS was 1.42 ± 0.05μg/ml and 1.66 ± 0.07μg/ml respectively. The increase in solubility in case of ZBLNS and ZBSNS was almost 5-folds higher than the ZB. According to Ostwald–Freundlich equation, saturation solubility is also dependent on the interfacial tension σ, i.e. the interfacial energy G (G = σ * A) where A is the surface area of the particle. Differences in interfacial energy are also a reason for the differences in saturation solubility of polymorphic forms (Muller RH and Peters K., 1998). The higher surface energy (by virtue of their higher surface area) of nanosuspensions is responsible for higher saturation solubility. Increase in the saturation solubility can also be explained by the possible creation of high energy surfaces when disrupting the more or less ideal drug microcrystals to nanoparticles. This in turn increases the exposure of the inner hydrophobic surfaces of the drug crystal to the aqueous dispersion medium.

In another way, increase in saturation solubility of the drug when formulated as nanosuspension can also be explained by Fick's law. There exists a high concentration gradient between the surface and the bulk solution due to the increased solubility near the particle surface. This enhanced concentration gradient, with agreement to Fick's law, should result in an increased mass transfer away from the particle surface (Kipp JE., 2004). As the particle diameter decreases, its surface area to volume ratio increases inversely, further leading to an increased dissolution rate.

In vitro release studies

ZB as dispersion form in pH 7.4 PB showed 98.91 ± 0.73% dissolution in about 90 min. According to Ostwald–Freundlich and the Kelvin equations (Grant DJW et al., 1995), the dissolution pressure increases due to the strong curvature of the particles leading to increase in saturation solubility. Further as per Noyes–Whitney, this increase in dissolution pressure leads to a further increase in dissolution rate in addition to the gain by an increased surface area.

The release profiles clearly indicated the faster dissolution rate of ZB in nanosuspension forms. Enhancement in the dissolution rate can be attributed to the increase in the surface area after

nanosizing the drug crystals. Further, this high surface area of the drug nanocrystal has been adsorbed with the hydrophilic copolymer poloxamer 407, and hence its hydrophilicity is expected to improve. These factors ultimately lead to the decrease in contact angle and hence increase in the dissolution rate. The release profiles of ZB dispersion and both the nanosuspension were best fitted into the Higuchi equation. The comparative t_{25}, t_{50} and t_{90} values for plain ZB dispersion and the nanosuspension formulations are given in table 8.6.

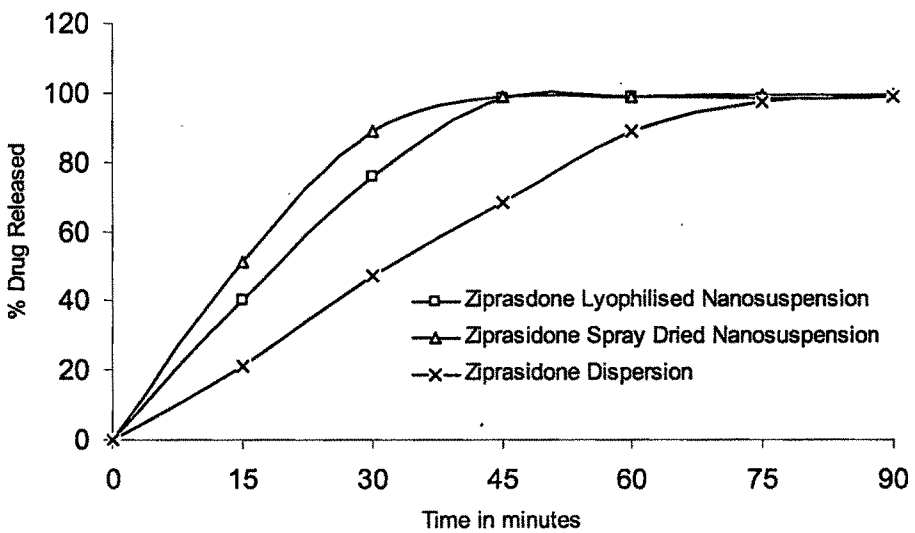

FIGURE 8.6: In vitro diffusion of Ziprasidone from the Ziprasidone nanosuspension in phosphate buffer pH 7.4 containing 2% sodium lauryl sulphate

Parameter	Time in minutes		
	Ziprasidone dispersion	Ziprasidone Lyophilized nanosuspension	Ziprasidone Spray Dried nanosuspension
t_{25}	17.08 ± 1.88	9.92 ± 1.26	7.76 ± 0.94
t_{50}	32.38 ± 2.15	18.53 ± 1.91	15.42 ± 1.25
t_{90}	63.81 ± 2.56	37.46 ± 1.21	34.02 ± 2.06

Table 8.6: Comparative t_{25} ± S.D (time taken for 25% ziprasidone to be released) t_{50} values (time taken for 50% ziprasidone to be released) and t_{90} (time taken for 90% ziprasidone to be released) of ziprasidone dispersion and both the nanosuspension formulations

Stability studies

Effect of temperature on particle size

The particle size was found to increase with the increasing time duration of storage, as a result of particle aggregation. Mean particle diameter of the ZB nanosuspensions stored at 40°C increased from 309 ± 3.22nm to 887 ± 7.59nm in 6 months, whereas, for samples stored at 4°C and 30°C, it increased only to 509 ± 4.77nm and 629 ± 6.51nm respectively (Figure 8.7). Apart from the particle diameter, the sedimentation velocity of the particles also increased in all the stability samples. However, the sedimentation was not harmful, as simple shaking again resulted in a homogenous nanodispersion. This phenomenon was also observed by Huettenrauch and co workers (Huettenrauch R and Moeller U., 1983) during their study on the milling of sulfathiazole

The observed particle size growth can be due to several reasons. As a consequence of increase in the input energy provided by the successively higher temperatures, there may be destabilization of the nanosuspension dispersions. This input energy increases the kinetic energy of the particles contributing to increased inter-particle collision and ultimately result in aggregation. Crystal growth in nanosuspensions can also be due to Ostwald ripening, which is mainly due to the differences in saturation solubility above the surface of differently sized

crystals and sufficiently high changes in solubility with temperature changes. The surfactant poloxamer used in this study is characterized with reduced aqueous solubility at higher temperatures, which can lead to particle aggregation at higher temperatures. Cleavage of hydrogen bonds between the hydrated polymer and water occurs at higher temperatures, leading to formation of visible polymer aggregates ("cloud point").

The contact points between particles have a high negative (concave) radius of curvature according to Ostwald – Freunlich equation (Kipp JE., 2004), and thus have a lower solubility than convex surfaces. This leads to solute buildup at these contact points and ultimately to the "knitting" together of particles (caking). Secondary nucleation occurs in a supersaturated solution from crystals of the solute already present in the crystallization medium. Changes in the temperature may result in dissolution of some drug at higher temperatures and recrystallize from a seeded supersaturated medium upon cooling (Kipp JE., 2004).

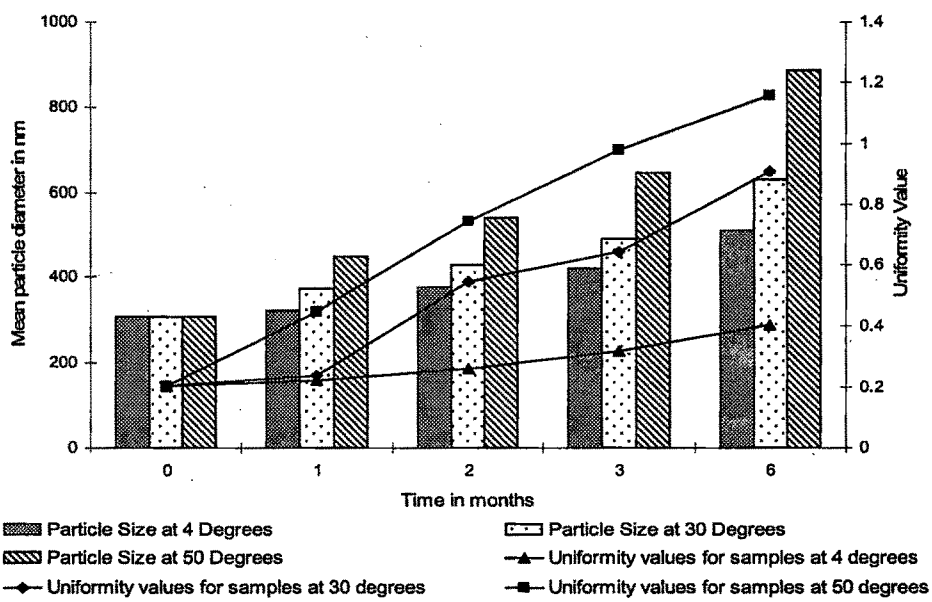

FIGURE 8.7: Mean particle Diameter of ziprasidone nanosuspension dispersion stored at different temperatures in dark condition.

Effect of storage temperature on zeta potential

Initial zeta potential of the ZB nanosuspension dispersion was determined to be -17.2 mV. Upon storage, there was a drop in the zeta potential of nanosuspensions. The zeta potential changes were most prominent in the samples stored at 40°C followed by samples at 30°C and 4°C. The zeta potential of ZB nanosuspensions stored at 40°C increased from -17.2mV to + 9.77mV in 6 months, whereas for samples stored at 4°C and 30°C, it increased to 0.93mV and -6.83mV respectively (Figure 8.7).

In the process of formulating a stable suspension, the potential energy created at the interface between the solid surface and the surrounding medium must be reduced by adding surface-active agents. Surface stabilization can be accomplished by either charged surfactants (anionic or cationic) or non–ionic polymers. Charged surfactants act by migration to the solid–liquid interface and build an electrostatic barrier to particle agglomeration. Non-ionic stabilizers also attach their hydrophobic domains at multiple sites on the particle surface. There is a low probability that these hydrophobic moieties will detach from the particle surface at room temperature, consequently providing a strong surface affinity (Alexandridis P and Hatton TA, 1995). Further, these non-ionic surfactants create a hydration zone, a layer of tightly bound water molecules around each particle. When two particles meet, work is required to dislodge this water layer because of osmotic forces, hence preventing particle agglomeration.

A system is considered stable if the electrostatic repulsion dominates the attractive van der Waals forces. When the kinetic energy of the particle is high enough to overcome the barrier of electrostatic repulsion, they undergo collision. Increase in temperature usually leads to increase in kinetic energy of a system, which in combination with a reduction in zeta potential leads to the aggregation of nanosuspension (Freitas C and Muller RH., 1998). Importantly, the probable implications of such variations in zeta potential values at storage conditions on the in vivo behavior of nanosuspensions cannot be ruled out.

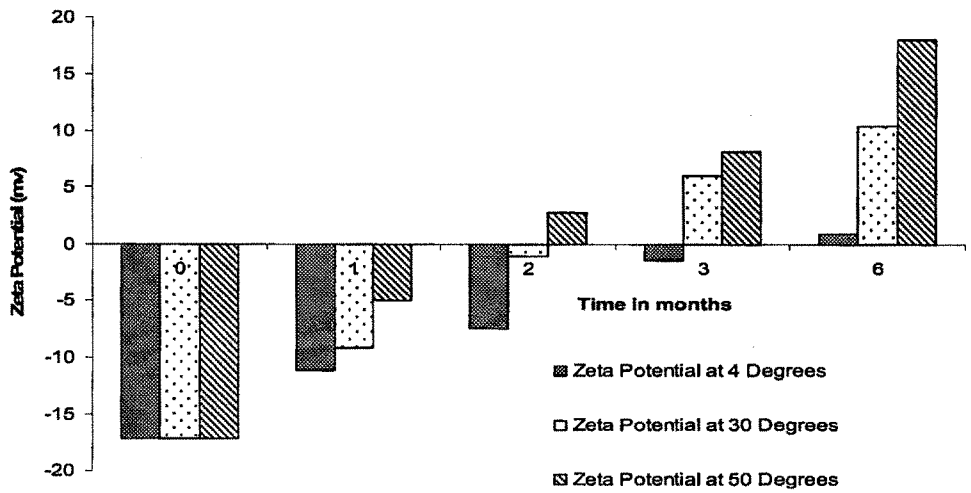

FIGURE 8.8: Zeta potential of ziprasidone nanosuspension dispersion stored at different temperatures in dark condition.

The stability data for ZBLNS and ZBSNS in powder state are shown in table 8.7 and 8.8 respectively. There was no significant change in the particle size of ZBLNS at 4°C (initial 309nm ± 4.31nm to 358nm ± 4.06nm), 30°C (initial 309nm ± 4.31nm to 374nm ± 3.56nm) and 40°C (initial 309nm ± 4.31nm to 403nm ± 4.02nm) in the after six months. Similar trend were observed with the stability samples of ZBSNS. There was no significant particle size growth in the powder state in all the three temperatures studied (initial 309nm ± 4.31nm to 366nm ± 4.20nm at 4°C; initial 309nm ± 4.31nm to 382nm ± 4.12nm; initial 309nm ± 4.31nm to 410nm ± 3.64nm). There was no significant change from the initial release pattern during the time period studied. The time required for reconstitution was almost similar at both the temperatures throughout the time period studied (14 to 23 seconds).

In vitro release studies were carried out for the microspheres removed after 1, 2, 3 and 6 months and compared with the initial in vitro release profile. To study the variability in dissolution data, the value of difference factor (f_1) and similarity factor (f_2) were calculated using the Moore and Flanner equation (Saranadasa H and Krishnamoorthy K., 2005). Moore and co workers used a simple model independent approach which utilizes a difference factor

(f_1) and similarity factor (f_2) to compare dissolution profiles (Moore JW and Flanner HH., 1996). The difference factor (f_1) calculates the percent (%) difference between the two curves at each time point and is a measurement of the relative error between the two curves. The similarity factor (f_2) is a logarithmic reciprocal square root transformation of the sum of squared error and is a measurement of the similarity in the percent (%) dissolution between the two curves. For curves to be considered similar, f_1 values should be close to 0, and f_2 values should be close to 100. Generally, f_1 values up to 15 (0-15) and f_2 values greater than 50 (50-100) ensure sameness or equivalence of the two curves and, thus, of the performance of the test and reference products.

In the present study, the values of the difference factor (f_1) were 0.8 to 4.7 indicating low difference between the initial in vitro release pattern and the in vitro pattern on storage. Further, the values of the similarity factor (f_2) were 74.6 to 96.2 indicating significant similarity between the initial in vitro release pattern and the in vitro pattern on storage

Time (Months)	Samples Stored at 4°C				Samples Stored at 30°C				Samples Stored at 40°C			
	Mean Particle Size Diameter (nm ± S.D)	Time for reconstitution (seconds ± S.D)	In vitro release		Mean Particle Size Diameter (nm ± S.D)	Time for reconstitution (seconds ± S.D)	In vitro release		Mean Particle Size Diameter (nm ± S.D)	Time for reconstitution (seconds ± S.D)	In vitro release	
			F1	F2			F1	F2			F1	F2
1	315 ± 4.31	15 ± 3.35	1.0	96.2	323 ± 5.24	19 ± 2.31	1.7	92.7	346 ± 5.23	20 ± 1.56	0.8	93.6
2	332 ± 5.21	18 ± 2.28	1.9	90.2	336 ± 4.86	20 ± 2.06	2.0	89.1	355 ± 4.49	22 ± 1.94	1.9	87.7
3	346 ± 6.08	17 ± 2.98	1.8	91.1	348 ± 4.22	20 ± 1.88	2.2	86.4	371 ± 5.03	23 ± 2.02	2.4	85.4
6	358 ± 4.06	20 ± 2.54	1.9	90.2	374 ± 3.56	22 ± 1.40	2.8	84.0	403 ± 4.02	23 ± 1.66	4.4	77.7

Table 8.7: Stability data for lyophilized ziprasidone nanosuspension (in the powder form)

Initial Particle Size Diameter 310 ± 3.87 nm

Initial time for reconstitution 15 ± 2.50 seconds

Time (Months)	Samples Stored at 4°C				Samples Stored at 30°C				Samples Stored at 40°C			
	Mean Particle Size Diameter (nm ± S.D)	Time for reconstitution (seconds ± S.D)	In vitro release		Mean Particle Size Diameter (nm ± S.D)	Time for reconstitution (seconds ± S.D)	In vitro release		Mean Particle Size Diameter (nm ± S.D)	Time for reconstitution (seconds ± S.D)	In vitro release	
			F1	F2			F1	F2			F1	F2
1	324 ± 3.98	14 ± 2.26	1.2	94.8	328 ± 5.06	17 ± 2.54	1.5	90.0	334 ± 5.00	16 ± 2.20	1.8	92.6
2	339 ± 4.08	16 ± 3.32	2.1	88.1	341 ± 4.46	18 ± 3.24	1.8	87.0	356 ± 4.36	16 ± 1.62	2.4	83.5
3	351 ± 3.52	16 ± 2.28	2.3	84.3	359 ± 3.56	18 ± 2.64	1.8	86.5	382 ± 4.02	18 ± 1.98	3.5	79.5
6	366 ± 4.20	17 ± 3.06	2.3	84.0	382 ± 4.12	20 ± 3.04	2.6	80.0	410 ± 3.64	18 ± 1.66	4.7	74.6

Table 8.8: Stability data for spray dried ziprasidone nanosuspension (in powder form)

Initial Particle Size Diameter 317 ± 4.28 nm

Initial time for reconstitution 13 ± 1.95 seconds

8.4 CONCLUSION

Pearl milling of ZB for 8 hours in the presence of poloxamer 407 as surfactant using zirconium oxide beads (75:25 ratio of size 0.4- 0.7mm: 1.2-1.4mm) yielded nanoparticles of smallest size. The nanosuspension dispersions can be successfully converted into the powder form by either lyophilization or by spray drying to increase the shelf life. There was a change in the crystallinity of ZB after conversion into nanosuspension state. Electrolyte flocculation test revealed that the nanosuspension formulations tended to agglomerate in electrolyte concentrations beyond 0.3M sodium sulphate. The nanosuspension forms of ziprasidone improved its solubility and dissolution in vitro. These encouraging results reveal the possible potential use of these nanosuspensions as alternative parenteral dosage forms to the existing marketed ziprasidone injection.

8.5 REFERENCES

Alexandridis P, Hatton TA, Poly (ethylene oxide) – poly (propylene oxide) – poly (ethylene oxide) block copolymer surfactants in aqueous solutions and at interfaces: thermodynamics, structure, dynamics, and modeling (review), *Colloids Surf. A: Physicochem. Eng. Aspects*, 1995, 96, 1–46.

Brock CP, Schweizer WB, Dunitz JD, On the validity of Wallach's rule: on the density and stability of racemic crystals compared with their chiral counterparts, *J. Am. Chem. Soc.* 1991, 113, 9811–9820.

Byrn SR, Pfeiffer RR, Stowell JG, Solid State Chemistry of Drugs, 2nd ed. SSCI, Lafayette, IN, 1999, pp. 8.

Coppola D, NanoCrystal technology targets poorly water-soluble drugs, *Pharmaceutical Technology*, 2003, 11, 20.

Czekai DA, Reed RG, Apparatus for sanitary wet milling, *US Patent Application 2004/0026546 A1* April 26, 2001

Font J, Muntasell J, Cesari E, Amorphization of organic compounds by ball milling, *Mater. Res. Bull.*, 1997, 32, 1691– 1696.

Freitas C, Muller RH, Effect of light and temperature on zeta potential and physical stability in solid lipid nanoparticle (SLN™) dispersions, *International Journal of Pharmaceutics*, 1998, 168, 221–229.

Grant DJW, Brittian HG, In: Brittian, H.G. (Ed.), Physical Characterization of Pharmaceutical Solids, 1995, Marcel Dekker, New York.

Huang SK, Martin FJ, Jay G, Extravasation and transcytosis of liposomes in Kaposi's sarcoma – like dermal lesions of transgenic mice bearing HIV Tat gene, *Am J Pathol.*,1993, 143, 10-14.

Huettenrauch R, Moeller U, Molecular galenics. Part 73. Correlation between the degree of order and the wettability of solids, *Pharmazie*, 1983, 38, 198.

Keck C.M, Muller RH, Drug nanocrystals of poorly soluble drugs produced by high pressure homogenization, *European Journal of Pharmaceutics and Biopharmaceutics*, 2006, 62, 3–16.

Kipp JE, The role of solid nanoparticle technology in the parenteral delivery of poorly water-soluble drugs, *International Journal of Pharmaceutics*, 2004, 284, 109–122.

Kitaigorodkii, 1961. Organic Chemical Crystallography. Consultants Bureau, New York.

Liversidge GG, Cundy KC, Bishop JF, Czekal DA, US Patent 5,145,684 (September 8, 1992).

Liversidge ME, Liversidge GG, Cooper E, Nanosizing: a formulation approach for poorly-water-soluble compounds, *Eur. J. Pharm Sci.* 2003, 18, 113–120.

Moore J W, Flanner HH, "Mathematical Comparison of Dissolution Profiles," *Pharmaceutical Technology*, 1996, 20, 64-74.

Muller RH, Peters K, Nanosuspensions for the formulation of poorly soluble drugs I. Preparation by a size-reduction technique, *International Journal of Pharmaceutics*, 1998, 160, 229–237.

Otsuka M, Kaneniwa N, Effect of seed crystals on solidstate transformation of polymorphs of chloramphenicol palmitate during grinding, *J. Pharm. Sci.* 1986, 75, 506–511.

Peters K, Leitzke S, Diederichs JE, Borner K, Hahn H, Muller RH, Ehlers S, Preparation of a clofazimine nanosuspension for intravenous use and evaluation of its therapeutic efficacy in murine Mycobacterium avium infection, *J. Antimicrob.Chemother.*, 2000, 45, 77–83.

Rogers TL, Johnston KP, Williams Iii RO, Solution-based particle formation of pharmaceutical powders by supercritical or compressed fluid CO_2 and cryogenic spray-freezing technologies, *Drug Development and Industrial Pharmacy*, 2001, 27, 1003-1015.

Saranadasa H, Krishnamoorthy K, A multivariate test for similarity of two dissolution profiles, *Journal of Biopharmaceutical Statistics*, 2005, 15, 265–278.

Sarkari M, Brown JN, Chen X, Swinnea S, Williams Iii RO, Johnston KP, Enhanced drug dissolution using evaporative precipitation into aqueous solution, *International Journal of Pharmaceutics*, 2002, 243, 17-31.

Saupe A, Wissing SA, Lenk A, Schmidt C, Muller RH, Solid Lipid Nanoparticles (SLN) and Nanostructured Lipid Carriers (NLC) – Structural investigations on two different carrier systems, *Bio-Medical Materials and Engineering*, 2005, 15, 393-402.

Subramanian N, Murthy RSR, Use of electrolyte induced flocculation technique for an in vitro steric stability study of steric study of steric stabilized liposome formulations, *Pharmazie,* 2003, 59, 74-76.

Troster, S. D., Kreuter, J., 1992. Influence of the surface properties of low contact angle surfactants on the body distribution of 14-C-poly (methyl methacrylate) nanoparticles. J. Microencapsul. 9, 19–28.

Verhoff F, Pace GW, Snow RA, Millar F, Milled particles, *US patent no 6,634,576,* October 12, 2003.

Ward GH, Schultz RK, Process-induced crystallinity changes in albuterol sulfate and its effect on powder physical stability, *Pharm. Res.* 1995, 12, 773–779.

Willart JF, De Gusseme A, Hemon S, Odou G, Danede F, Descamps M, Direct crystal to glass transformation of trehalose induced by ball milling, *Solid State Commun.*, 2001, 119, 501–505.